

Present performance and future upgrades of the AURIGA capacitive readout

Andrea Vinante (for the AURIGA Collaboration)

Dipartimento di Fisica, Università di Trento and INFN, Gruppo Collegato di Trento,
Sezione di Padova, I-38050 Povo, Italy

E-mail: vinante@science.unitn.it

Received 27 September 2005, in final form 23 December 2005

Published 24 March 2006

Online at stacks.iop.org/CQG/23/S103

Abstract

The resonant bar gravitational wave detector AURIGA is taking data for its second run at $T = 4.5$ K. The readout has been largely upgraded with respect to the previous run. In particular, we have realized a 3-mode detection scheme by tuning the high- Q resonance of the electrical readout to the mechanical modes of bar and transducer. Moreover, a low noise two-stage SQUID amplifier has been implemented. Thanks to these improvements, the bandwidth has been largely increased and the strain sensitivity is now better than 10^{-20} Hz $^{-1/2}$ over more than 100 Hz. In this paper, we describe a 3-mode model of the detector, which allows us to distinguish between the different noise contributions. Some possible upgrades are discussed.

PACS numbers: 04.80.Nn, 05.40.–a, 85.25.Dq

(Some figures in this article are in colour only in the electronic version)

1. Introduction

The main limitation of the present operating resonant gravitational wave (GW) detectors is the relatively narrow bandwidth. Up to now, bandwidths not larger than a few tens Hz have practically been achieved [1]. It must be noted that this limitation is not intrinsic to a resonant detector, but is instead related to the poor performance of the readout. In particular, two principal factors have prevented the resonant detectors from achieving larger bandwidths. The first is the upper limit on the transducer efficiency, set by physical or technological constraints, like the breakdown bias field for a capacitive transducer. The second is the additive noise of the readout amplifier. For this reason, the recent efforts of the AURIGA group towards achieving a larger bandwidth have been focused mainly on two directions. First, we have increased the transducer efficiency, and hence the energy coupling between bar resonator and amplifier, by using a capacitive transducer with an electrical resonating matching line [2, 3]. Second, we

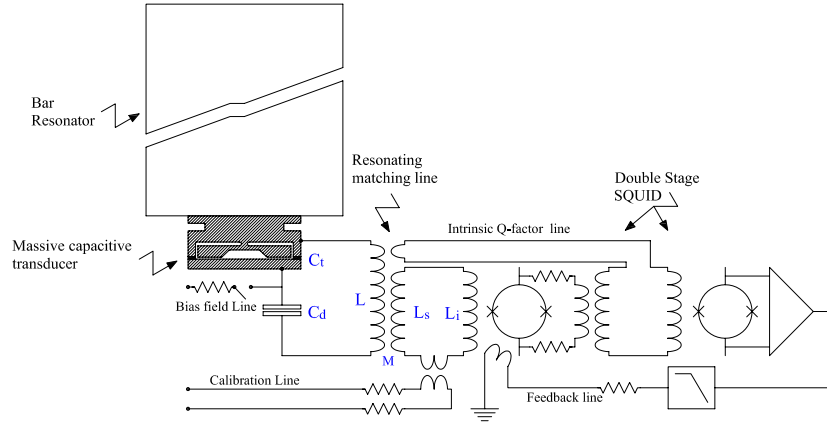


Figure 1. Scheme of the AURIGA readout.

Table 1. List of actual parameters used in the simulations.

Parameter	Symbol	Value
Bar effective mass	m_b	1150 kg
Bar length	l_b	2.94 m
Bar resonance frequency	$\nu_b = \omega_b/2\pi$	900 Hz
Bar quality factor	Q_b	4×10^6
Transducer effective mass	m_t	6.1 kg
Transducer resonance frequency	$\nu_t = \omega_t/2\pi$	898 Hz
Transducer quality factor	Q_t	1.5×10^6
Capacitor bias field	E	$7.5 \times 10^6 \text{ V m}^{-1}$
Transducer capacitance	C_t	8.45 nF
Decoupling capacitance	C_d	69.5 nF
Primary coil inductance	L	7.9 H
Secondary coil inductance	L_s	3.48 μH
Transformer mutual inductance	M	4.5 mH
Electrical resonance frequency	$\nu_{el} = \omega_{el}/2\pi$	941 Hz
Electrical quality factor	Q_{el}	4.5×10^5
SQUID input inductance	L_i	1.48 μH
SQUID additive noise energy	$\epsilon_{ii} \equiv L_i S_{ii}/2$	$60 + 140 \times T(\text{K}) \hbar$
SQUID back action energy	$\epsilon_{vv} \equiv S_{vv}/(2\omega^2 L_i)$	$20 \times T(\text{K}) \hbar$

have reduced as much as possible the amplifier noise by means of two-stage SQUID systems [4–6]. In consequence of these efforts, the AURIGA detector is now taking data for its second scientific run with a bandwidth significantly larger than that in the previous run [3].

In this paper, the main features of the new readout will be reviewed. The actual experimental sensitivity will be compared to the predictions of a 3-mode model of the detector. Finally, some possible upgrades, which could be implemented in the mid-term, will be discussed, in particular in view of cooling down the detector to ultracryogenic temperatures.

2. Three-mode model

A simplified scheme of the AURIGA readout is shown in figure 1. The actual values of the parameters used in the model are listed in table 1. The bar displacement is sensed by a

capacitive resonant transducer [7]. Its main element is a mechanical resonator attached to a face of the bar, which serves as a mechanical amplification stage. Bar and resonant transducer are modelled as two coupled harmonic resonators with effective masses m_b and m_t , uncoupled resonance frequencies $\nu_b = \omega_b/2\pi$, $\nu_t = \omega_t/2\pi$ and quality factors Q_b , Q_t , with $\nu_b \approx \nu_t$ and $m_t \ll m_b$. The displacement of the transducer resonator x_t , with respect to that of the bar x_b , modulates a capacitor, biased by a dc electric field E . The mechanical vibration is converted to a voltage $E(x_t - x_b)$ across the capacitor. A second decoupling capacitor with capacitance $C_d \gg C_t$ is required to keep the charge on the transducer. The transducer output electrical signal is read by a SQUID current amplifier, of input inductance L_i . A superconducting transformer, with primary coil, secondary coil and mutual inductance given respectively by L , L_s and M , is interposed as an electrical impedance matching stage. The electrical circuit shows a LC resonance with resonance angular frequency $\omega_{el} = 1/\sqrt{L_r C}$ and quality factor Q_{el} , where $L_r = L - M^2/(L_s + L_i)$ is the reduced inductance of the transformer primary coil and $1/C = 1/C_t + 1/C_d$ is the effective capacitance.

In the present AURIGA run, we have succeeded for the first time in tuning the frequency of the electrical LC mode close to the frequency of the mechanical modes of bar and transducer. The main consequence is that the transducer efficiency around the mechanical modes is largely increased with respect to the untuned readout [2]. Actually, a capacitive transducer with the tuned electrical mode behaves as a two-mode transducer. When coupled to the bar, it realizes a system with three effective modes [8]. A full three-mode model of detector is then required.

The equations of motion of the system can be written in the form

$$\begin{aligned}
m_b \ddot{x}_b + \frac{m_b \omega_b}{Q_b} \dot{x}_b + m_b \omega_b^2 x_b + \frac{m_t \omega_t}{Q_t} (\dot{x}_b - \dot{x}_t) + m_t \omega_t^2 (x_b - x_t) + Eq &= F_{\text{ext}} + F_{\text{th-b}} \\
m_t \ddot{x}_t + \frac{m_t \omega_t}{Q_t} (\dot{x}_t - \dot{x}_b) + m_t \omega_t^2 (x_t - x_b) - Eq &= F_{\text{th-t}} \\
L_r \ddot{q} + \frac{L_r \omega_{el}}{Q_{el}} \dot{q} + \frac{q}{C} + E(x_t - x_b) &= V_{\text{th}} - \frac{M}{(L_i + L_s)} V_n \\
(L_i + L_s) \dot{I}_{\text{SQ}} + M \dot{q} &= V_n \\
V_{\text{SQ}} &= A(I_{\text{SQ}} + I_n).
\end{aligned} \tag{1}$$

x_b , x_t , q , I_{SQ} and V_{SQ} are, respectively, the displacement of the face of the bar and of the transducer resonator, the charge induced on the capacitor, the input current and output voltage of the SQUID. $F_{\text{th-b}}$, $F_{\text{th-t}}$ and V_{th} are the thermal noise sources of the three resonators, with one-sided spectral densities respectively $4k_B T m_b \omega_b / Q_b$, $4k_B T m_t \omega_t / Q_t$ and $4k_B T L_r \omega_{el} / Q_{el}$. F_{ext} is the external force acting on the bar resonator. V_n , I_n are the back action voltage noise and additive current noise of the SQUID, modelled as current amplifier, with spectral densities S_{vv} and S_{ii} [5, 6]. A is the SQUID gain.

Equations (1) describe a system with three normal modes, linear superposition of the three uncoupled resonators, two mechanicals and one electrical. The third equation of (1), describing the electrical resonator, can be reduced to the equation of an equivalent mechanical resonator, with equivalent displacement $x_{el} = q \omega_{el}^2 / E L_r$ and equivalent mass $m_{el} = E^2 / (\omega_{el}^4 L_r) \approx 12$ g. Thus, the masses of the three modes, m_b , m_t and m_{el} , are roughly stepwise decreasing, as required for an optimally matched multimode transducer [9].

An important feature of multimode transducers such as AURIGA's one is that the mass of the transducer resonator can be made much larger than in a monomode transducer because less mechanical gain is needed. This step is essential in obtaining a higher bandwidth. In fact, as shown in [9], the maximum bandwidth, which can be eventually achieved under optimal matching conditions, is given roughly by $\Delta \nu_{\text{max}} \approx 2\nu_b \sqrt{m_t/m_b}$. Indeed the effective

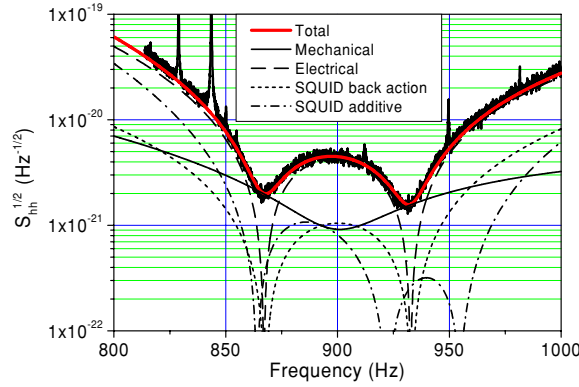


Figure 2. Present one-sided strain sensitivity of the AURIGA detector, operated at $T = 4.5$ K, compared to predictions of the three-mode model. The different noise contributions are also plotted.

transducer mass in the present run of AURIGA is about 20 times higher than in the previous run.

The main drawback of tuning the electrical mode is that the electrical thermal noise and the SQUID back action noise become important factors in determining the actual bandwidth. In practice, this leads to a severe constraint on the electrical quality factor Q_{el} , which must be at least of the order of the mechanical quality factor ($\approx 10^6$) in order to achieve a significant bandwidth improvement [3]. To achieve this goal, great care has been taken to minimize all possible sources of dissipation located in the electrical circuit and in the input circuit of the SQUID amplifier.

Equations (1) can be numerically solved in the frequency domain, allowing a precise evaluation of the dynamical and noise properties of the system. In particular, we can predict the detector strain sensitivity through the following steps.

- (i) The total SQUID output voltage noise $S_{VV}(\omega)$ is calculated solving equations (1) with $F_{ext} = 0$.
- (ii) The mechanical response function $T(\omega)$, i.e. the ratio between the SQUID output voltage and a unitary force $F_{ext}(\omega) = 1$ is calculated by solving equations (1) without noise terms. The force sensitivity is then calculated as $S_{ff}(\omega) = S_{VV}(\omega)/|T(\omega)|^2$.
- (iii) The force noise is converted in gravitational strain noise through the relation [10]

$$S_{hh}(\omega) = S_{ff}(\omega) \left(\frac{\pi}{2m_b\omega^2 l_b} \right)^2, \quad (2)$$

where l_b is the physical length of the bar.

Finally, we briefly discuss some limitations of the model. First, we have neglected the presence of other spurious mechanical modes weakly coupled to the system (for instance two spurious modes exist at 828 Hz and 843 Hz, see figure 2). Second, equation (2) is strictly valid only for a ideal thin bar, but some small corrections are expected for a real bar such as AURIGA. For these reasons, in the near future the model will be refined and an overall finite element method (FEM) simulation of the whole detector will be performed.

3. Experimental setup

The bar is a 2.3 ton, 3 m long cylinder made of Al5056. The transducer is a mushroom-shaped Al5056 resonator, whose fundamental flexural mode is tuned to the fundamental longitudinal

mode of the bar [7, 11]. The effective mass of the bar mode m_b is expected to be half the total mass of the bar. This assumption is supported by experimental tests performed at room temperature. Other mechanical parameters have been estimated by means of measurements performed *in situ* at very low bias field. In this limit, the mechanical system is completely decoupled from the electrical mode and from the SQUID and reduces to a system with two normal modes, with frequencies ν_- and ν_+ and quality factors Q_- and Q_+ . If $m_t \ll m_b$ and $\nu_b \approx \nu_t$ one can easily derive from the model the following relations:

$$\nu_+ - \nu_- = \nu_b \sqrt{m_t/m_b}, \quad \nu_+/Q_+ + \nu_-/Q_- = \nu_b/Q_b + \nu_t/Q_t. \quad (3)$$

The first of equations (3) allows us to experimentally infer the effective transducer mass m_t from the frequency splitting of the modes. The second equation allows us to estimate the uncoupled quality factor of the bar mode Q_b from the values of Q_+ and Q_- , measured *in situ*, and the value of Q_t , measured in previous bench tests [2].

The mushroom resonator is the ground plate of the transducer capacitor. The opposite high voltage plate is rigidly attached to the resonant transducer base by means of 40 μm PTFE Teflon spacers. The superconducting transformer is housed in a separate superconducting SnPb electroplated copper box, attached to the transducer by means of decoupling suspensions. The transformer has a very high geometrical coupling factor $k = M/\sqrt{LL_s} = 0.86$, and very small stray capacitance, of order 10 pF, obtained by means of a multisector primary coil [12]. Two separate boxes, also vibrationally decoupled by means of calibrated suspensions, house respectively the decoupling PTFE Teflon capacitor C_d and the cryogenic switch. The switch, based on a commercial reed relay, is another novel feature of the AURIGA readout. When closed, it allows us to quickly charge or discharge the transducer. When open, it provides a very effective decoupling from room temperature wiring, because of its very small capacitance of 0.1 pF. In particular the electrical quality factor is practically not affected by the presence of the charging line.

The SQUID is a two-stage dc SQUID amplifier, operated in conventional flux-locked loop mode [4]. The two SQUID units are housed in separate compartments of the transformer box. In the two-stage configuration the signal from the first SQUID (sensor SQUID) is amplified by a second SQUID (amplifier SQUID) in order to make the noise of the room temperature electronics negligible and to achieve the intrinsic noise of the sensor SQUID. This system has been extensively characterized in previous articles [5, 6]. In particular, both additive current noise and back action voltage noise of the SQUID, modelled as current amplifier, are expected to scale linearly with temperature, according to theoretical predictions. Recent measurements have shown that this is true for both noise sources down to about 200 mK, where a saturation of the effective SQUID temperature occurs, perhaps due to the hot electron effect [4, 13]. A more precise noise characterization of the SQUID used includes an additional $1/f$ term in the additive noise, which has been estimated as $60\hbar$ at 900 Hz and nearly independent of temperature [5]. Moreover, a correlation term S_{iv} should exist, but it is not as well characterized as S_{ii} and S_{vv} . We have checked that a correlation term like that expected by theoretical models [14] would not produce significant effects on the AURIGA sensitivity within the present experimental setup. Therefore, for simplicity we neglect it.

Several additional features have been developed in order to ensure stable and reliable operation of the SQUID when coupled to the high- Q resonant input circuit, and to allow an accurate characterization of the detector.

- (i) An RC filter placed between the feedback line and the input coil is used as a cold damping network [15]. The typical quality factors of the main normal modes of the system are reduced during normal operation to values between 300 and 6000. Several practical advantages are obtained. In particular, the cold damped quality factor of the modes Q_{cd}

is stabilized and negative Q instabilities, which are known to affect SQUID-resonator systems, are avoided. It is worth noting that the damping is obtained by means of a feedback loop, so that it is not directly related to a real dissipation, and the signal-to-noise ratio of the detector is not affected. For this reason, we do not consider the cold damping in the equations (1), where instead the intrinsic Q -factor, related only to the passive dissipations, must be used.

- (ii) A new feedback electronics has been developed. In particular, a two-pole integrator has been implemented [16] and the feedback bandwidth has been enlarged to ≈ 100 kHz. In consequence, the slew rate has been increased by two orders of magnitude at frequencies below 200 Hz, where large interfering noise lines exist, due to high- Q resonances in the mechanical attenuation system. Moreover, dynamic range and linearity in the sensitivity band have been increased, and the time delay introduced by the SQUID electronics, which affects the detector timing accuracy, has been reduced to the order of a few μ s. Finally, an automatic reset circuit has been implemented, allowing a locking time close to 100%.
- (iii) A small pick-up coil, weakly coupled to the transformer primary coil, is inserted in the input circuit of the amplifier SQUID. It allows us to measure the intrinsic Q -factor of the normal modes, which is related only to the passive dissipation of the system. Details on the measurement method are reported in [3]. In particular, the uncoupled electrical Q -factor can be directly measured at zero bias field. The measured Q_{el} automatically includes dissipations located in the input circuit of the SQUID. Therefore, the corresponding thermal noise is included in the electrical thermal noise, while in previous articles it was treated as back action noise [5, 6]. The SQUID contribution to the electrical dissipation is estimated to be roughly 60% of total, because the electrical Q without the SQUID has been measured as 1.3×10^6 in separate bench tests. According to the adopted convention, one must include in S_{vv} only the residual SQUID back action that has been estimated in [6].
- (iv) A calibration coil is integrated in the input circuit of the sensor SQUID. It is coupled with a mutual inductance $M_{cal} = 6.4 \times 10^{-8}$ H to a pick-up coil of negligible inductance in series to the SQUID input coil L_i . The calibration coil allows the measurement of the equivalent impedance Z_{eq} seen from the SQUID port. Knowledge of Z_{eq} allows us to estimate the energy stored in the normal modes and to perform an energy calibration. Moreover, one can perform a model-independent check on the thermal behaviour of the detector noise [2, 3].

4. Present performance and future upgrades

Figure 2 shows the (one-sided) strain noise predicted by the model for the present AURIGA setup at $T = 4.5$ K, compared to the experimental curve. We will not discuss here the calibration procedure used to obtain the experimental curve, which is similar to that used in other experiments [10]; a complete report on the AURIGA calibration is in preparation. The curves agree to within less than 10% for all of the frequency range. The strain noise is better than 10^{-20} Hz $^{-1/2}$ over 110 Hz, compared with about 25 Hz for the previous run and about 40 Hz for other operating detectors [1]. The minimum detectable Fourier amplitude of a GW burst is $H_0 = 1.4 \times 10^{-22}$ Hz $^{-1}$. In figure 2, the different noise contributions are also plotted. At present, the electrical thermal noise is the main limiting factor, while the SQUID additive noise is practically negligible. Therefore, the overall curve presents only two minima, which correspond to the two zeros of the electrical noise transfer function. The zeros are placed at the frequencies of the mechanical normal modes at zero bias field, respectively $\nu_- = 866$ Hz and $\nu_+ = 931$ Hz.

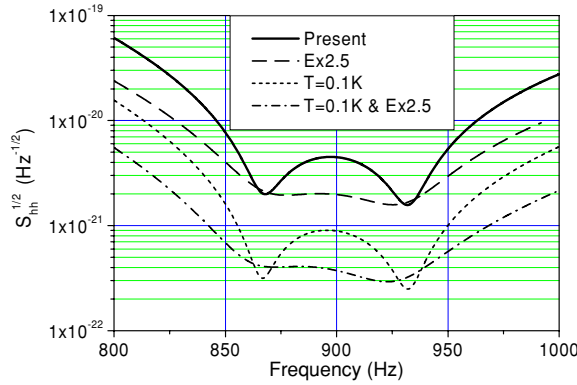


Figure 3. Predictions of the AURIGA sensitivity, corresponding to the following upgrades: increased bias field $E \times 2.5$, ultracryogenic operation $T = 0.1$ K, and both improvements together.

Several possible upgrades seem reasonable in the mid-term. The corresponding sensitivity curves are plotted in figure 3. First, one may try to reduce the electrical noise in order to obtain a flatter response and higher bandwidth. With the present matching conditions the electrical noise contribution scales roughly as $E^{-1} Q_{\text{el}}^{-1/2}$. Thus, one needs either to increase E or Q_{el} . The breakdown bias field could be increased at least by a factor 10 by means of a proper conditioning of the capacitor surface [17]. In the simulations we have considered a factor 2.5. On the other hand, increasing Q_{el} seems a more difficult task. However, since a substantial fraction of the electrical dissipation is located within the SQUID chip, an increase of Q_{el} up to a factor of 2 could be obtained by replacing the sensor SQUID with another device with smaller dissipation. This possibility is supported by recent dissipation measurements performed on other SQUID chips.

A second large improvement could be obtained by cooling the detector to ultracryogenic temperatures. In this case, one will fully exploit the practical absence of non-thermal noise contributions in the present readout. A temperature of 100 mK, as in the first AURIGA run, is a reasonable target. The 100 mK curves in figure 3 are obtained by assuming that Q -factors do not depend on temperature, and that electrical noise and mechanical noise scale with T . As regards the electrical noise, the scaling of the thermal noise in a high- Q resonator at ultracryogenic temperature has already been demonstrated [12]. Finally, the SQUID noise is assumed to saturate at a temperature of 200 mK, as observed in separate bench tests [13]. To take into account that roughly 60% of the electrical thermal noise is related to dissipations in the SQUID, and thus scales with the SQUID effective temperature [6], we have assumed an average temperature for the electrical thermal noise of 160 mK. The final predicted sensitivity of AURIGA at ultracryogenic temperature, with increased bias field, is of order $3\text{--}4 \times 10^{-22} \text{ Hz}^{-1/2}$ over about 80 Hz, with a minimum detectable Fourier amplitude of a GW burst $H_0 = 1.8 \times 10^{-23} \text{ Hz}^{-1}$.

5. Conclusions

The AURIGA detector has achieved in its second scientific run a significant improvement in bandwidth, thanks to the development of a three-mode detection scheme and a two-stage SQUID amplifier. However, a large potential reserve exists for further improvement that could be achieved without structural modification of the capacitive readout. The bandwidth can

be further increased by means of a moderate increase of the bias field. A large strain noise improvement of a factor of 7–8 over the whole bandwidth can be achieved by operating at ultracryogenic temperature, thanks to the thermal behaviour of the noise sources presently limiting the sensitivity.

References

- [1] Astone P *et al* 2003 *Phys. Rev. Lett.* **91** 111101
- [2] Zendri J P *et al* 2002 *Class. Quantum Grav.* **19** 1925–33
- [3] Baggio L *et al* 2005 *Phys. Rev. Lett.* **94** 241101
- [4] Mezzena R *et al* 2001 *Rev. Sci. Instrum.* **72** 3694–98
- [5] Vinante A *et al* 2001 *Appl. Phys. Lett.* **79** 2597–99
- [6] Falferi P *et al* 2003 *Appl. Phys. Lett.* **82** 931–33
- [7] Rapagnani P 1982 *Nuovo Cimento C* **5** 385
- [8] Tricarico P 1993 *Phys. Rev. D* **48** 241101
- [9] Richard J P 1984 *Phys. Rev. Lett.* **52** 165–7
- [10] McHugh M P *et al* 2005 *Class. Quantum Grav.* **22** 965–73
- [11] Marin A 2002 *PhD Thesis* Università di Padova, Italy
- [12] Vinante A *et al* 2005 *Rev. Sci. Instrum.* **76** 074501
- [13] Falferi P *et al* 2005 *Appl. Phys. Lett.* **88** 062505
- [14] Falferi P *et al* 2001 *J. Low Temp. Phys.* **123** 275–302
- [15] Vinante A *et al* 2001 *Physica C* **368** 176–80
- [16] Giffard R P 1980 *Proc. Conf. SQUID '80* ed H D Hahlbohm and H Lubbig (Berlin: de Gruyter) pp 445–71
- [17] Kobayashi S 1997 *IEEE Trans. Dielectr. Electr. Insul.* **4** 841